Stiffness of Contacts between Rough Surfaces

Sreekanth Akarapu,[1] Tristan Sharp,[1] and Mark O. Robbins[1]

[1]Department of Physics and Astronomy, Johns Hopkins University, 3400 N Charles Street, Baltimore, Maryland 21218, USA

(Received 5 November 2010; published 20 May 2011)

The effect of self-affine roughness on solid contact is examined with molecular dynamics and continuum calculations. The contact area and normal stiffness rise linearly with the applied load, and the load rises exponentially with decreasing separation between surfaces. Results for a wide range of roughness, system size, and Poisson ratio can be collapsed using Persson's contact theory for continuous elastic media. The compliance due to atomic-scale motion at the interface between solids has little effect on the area and normal stiffness, but can reduce the total transverse stiffness by orders of magnitude. The scaling of this effect with system size is discussed.

DOI: 10.1103/PhysRevLett.106.204301 PACS numbers: 46.55.+d, 62.20.Qp, 81.40.Pq

The presence of roughness on a wide range of length scales has profound effects on contact and friction between experimental surfaces. Under a broad range of conditions [1–6], the area of intimate contact between rough surfaces A_c is orders of magnitude smaller than the apparent surface area A_0. As discussed below, this provides the most common explanation for Amontons's laws that friction is proportional to load and independent of A_0. Because A_c is small, the interfacial region is very compliant. In applications from jet engine mounts to microelectromechanical systems, the interfacial compliance can significantly reduce the stiffness of joints formed by pressing two components together [1,7].

In this Letter, we examine the effect of surface roughness on the normal and transverse stiffness of contacts between elastic solids using molecular dynamics (MD) and continuum calculations. The results provide a numerical test of recent continuum theories [8,9] and their applicability to real solids. The contact area and normal stiffness approach continuum predictions rapidly as system size increases. Continuum theory also captures the internal deformations in solids under lateral forces, but the total transverse stiffness may be greatly reduced by atomic-scale displacements between contacting atoms on the opposing surfaces. This makes transverse stiffness a sensitive probe of the forces underlying friction and may help to explain unexpectedly small experimental values [10].

The topography of many surfaces can be described as a self-affine fractal [2,11]. Over a wide range of lengths, the root mean squared (rms) change in height dh over a lateral distance ℓ scales as a power law: $dh \sim \ell^H$, where the roughness or Hurst exponent H is typically between 0.5 and 0.9. Greenwood and Williamson (GW) considered the peaks of rough landscapes as independent asperities and found that A_c rose linearly with normal load F_N for nonadhesive surfaces [2]. This explains Amontons's laws if there is a constant shear stress at the interface. A linear scaling of area with load is also obtained from Persson's scaling theory, which includes elastic coupling between contacts approximately [3,12].

Dimensional analysis implies that the linear relation between load and area has the form

$$A_c E' = \kappa F_N / \sqrt{|\nabla h|^2}, \tag{1}$$

where a modulus like the contact modulus E' is the only dimensional quantity characterizing the elastic response, and the rms slope the simplest dimensionless quantity characterizing the roughness. Numerical solutions of the continuum equations [4,6] show that κ is near 2. Results for different H and Poisson ratio ν lie between the analytic predictions of GW, $\sqrt{2\pi} \sim 2.5$, and Persson, $\sqrt{8/\pi} \sim 1.6$. One advantage of Persson's model is that, as in numerical results, A_c/F_N is constant over a much larger range of loads than GW [13]. Another is that it captures [9] the power law scaling of correlations in contact and stress that was found in numerical studies [14,15].

The normal stiffness is related to the change in average surface separation u with load. Experiments [16,17] and calculations [5,8,18] show an exponential rise in load with decreasing u, $F_N = cA_0E' \exp[-u/\gamma h_{\rm rms}]$, where $h_{\rm rms}$ is the rms variation in surface height and γ a constant of order 1. Differentiating leads to an expression for the normal interfacial stiffness:

$$k_N^I = -dF_N/du = F_N/\gamma h_{\rm rms}. \tag{2}$$

For self-affine surfaces, this interfacial stiffness decreases as $h_{\rm rms}^{-1} \sim L^{-H}$ with increasing system size L. Our simulations test this scaling and show that γ is nearly constant. They also examine the connection between this normal stiffness and the transverse stiffness k_T^I measured at forces lower than the static friction [19].

We consider nonadhesive contact of a rigid rough solid and a flat elastic substrate. This can be mapped to contact of two rough, elastic solids in continuum theories [2,3]. The mapping is only approximate for atomic systems [20,21], but reduces the parameter space. Since thermal

fluctuations are usually ignored in continuum theory, we consider the zero temperature limit.

In our MD simulations, substrate atoms separated by r interact with a Lennard-Jones (LJ) potential: $U_{\mathrm{LJ}} = 4\epsilon[(\sigma/r)^{12} - (\sigma/r)^6]$, where ϵ and σ are the bonding energy and diameter. To speed calculations, the potential and force are interpolated smoothly to zero at $r_c = 1.8\sigma$ and energy minimization is used to find stable states [22]. Single-asperity simulations yield an effective contact modulus $E' = 63\epsilon/\sigma^3$ [20]. The substrate is face-centered-cubic and forms a cube of edge L with a (100) top surface. Periodic boundary conditions are applied in the plane of the top surface and the bottom is held fixed. Continuum calculations used the same substrate dimensions but obtained the displacements using a Green's function (GF) method [6] with the GF for an isotropic, continuous medium with Poisson ratio $\nu = 0$ or 0.35.

The rigid surface contained atoms on a square or triangular grid. The nearest-neighbor spacing d' was chosen to prevent commensurate locking with the substrate [23,24]. The interaction between substrate and rigid atoms is a LJ potential with length σ' truncated at the energy minimum, $2^{1/6}\sigma'$. This produces the purely repulsive interactions assumed in Persson's theory. Rigid atoms are displaced vertically to coincide with a self-affine fractal surface of the desired H. Surfaces with roughness on wavelengths from $l_{\mathrm{min}} = 5.9\sigma$ to $l_{\mathrm{max}} = L$ were generated as in Ref. [14]. The rms slope $\sqrt{|\nabla h|^2} = 0.1$ for the results shown. Consistent results were obtained for slopes from 0.05 to 0.15. Slopes of 0.2 or greater led to plastic deformation in MD simulations. Large slopes also led to plasticity in previous continuum calculations [5].

In all cases studied, A_c rises linearly with F_N. Moreover, the value of κ approaches previous continuum results [4,6] as system size increases. The stress and contact correlation functions from the MD calculations also show the same power law scaling with wave vector found in continuum calculations and Persson's theory [9,15].

Figure 1 shows the variation of F_N with interfacial separation u for several L and $H = 0.5$ and 0.8. In all cases, F_N rises exponentially over a range of loads that corresponds to fractional contact areas between 1% and 10%. Statistics are too poor at lower areas and nonlinear corrections to Eq. (1) are seen at larger areas [4]. The linear fits to all results have the same slope, corresponding to $\gamma = 0.48$, and best fit values for all H and L studied differ by less than 10% from this value. GF results were at the higher end of this range and showed no change as ν increased from 0 to 0.35. Earlier continuum calculations [5], elastic atomic calculations [18], and experiments [17] were consistent with $\gamma \approx 0.4$. This represents a compelling success of Persson's approach, and raises the question of whether γ may have a unique value in the thermodynamic, isotropic limit.

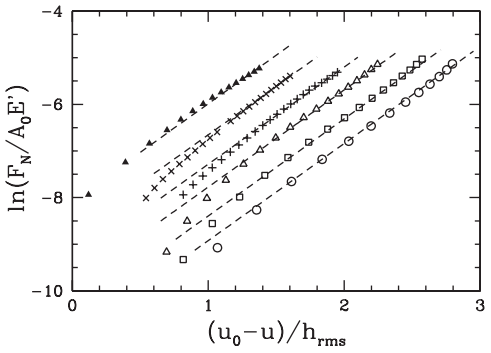

FIG. 1. Logarithm of load as a function of $(u_0 - u)/h_{\mathrm{rms}}$, and linear fits corresponding to $\gamma = 0.48$. The separation at first contact, u_0, is shifted slightly for each curve to prevent overlap. Atomistic results are for $H = 0.5$ with $L = 378.4\sigma$ (circles), 189.2σ (squares), and 94.6σ (triangles) and for $H = 0.8$ with $L = 189.2\sigma$ (pluses) and 94.6σ (crosses). Filled triangles are for a GF simulation with $L = 142.7\sigma$ and $\nu = 0$.

The normal stiffness from Eq. (2) includes a component from the increase in contact area with load as well as the change in force at fixed area. There is also an atomic-scale compliance k^{Ia} associated with changes in the separation between contacting atoms on opposing surfaces that is generally neglected in continuum theory. To isolate the stiffness associated with deformation within the substrate at fixed contact area k^{Is}, we applied constraints directly to the substrate atoms that contacted at a given load. The normal and transverse stiffness were obtained from the linear change in force produced by small, uniform normal or transverse displacements of these contacting atoms. The contribution from the bulk response was subtracted so that the stiffness reflects the change in surface separation u or transverse surface translation u_T. This approach is straightforward to implement in experiments and was found to be consistent with direct averaging of atomic separations.

Figure 2(a) shows the scaled normal interfacial stiffness $k_N^{Is} h_{\mathrm{rms}}/A_0 E'$ as a function of the dimensionless load F_N/A_0E' used to find the contacting atoms. Once again, results for all systems show the same behavior, and the stiffness rises linearly with load as predicted by Eq. (2). The points lie slightly above the dashed line corresponding to $\gamma = 0.48$ due to small deviations from the analytic form of Eq. (2). One might expect k_N^{Is} to be substantially less than the total stiffness because it does not include the stiffness from increases in contact area. However, the two quantities are nearly the same because newly contacting regions carry the smallest forces.

The incremental response of an ideal elastic solid does not depend on any preexisting deformation. This implies that we should obtain the same stiffness by displacing the same set of atoms on the initial undeformed surface. Direct evaluation of the stiffness in this way gave slightly lower values than Fig. 2, with the difference increasing from the numerical uncertainty to about 15% with increasing F_N.

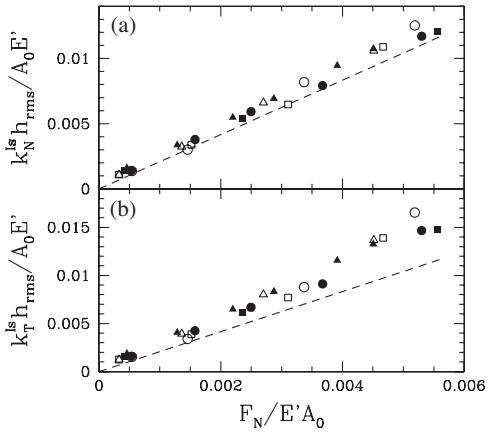

FIG. 2. The scaled (a) normal stiffness and (b) transverse stiffness as a function of F_N/A_0E'. Results are for $H = 0.5$ (open symbols) and $H = 0.8$ (filled symbols) with $L = 189.2\sigma$ (circles), $L = 94.6\sigma$ (squares), or $L = 47.3\sigma$ (triangles). Dashed lines have slope $1/\gamma$ with $\gamma = 0.48$.

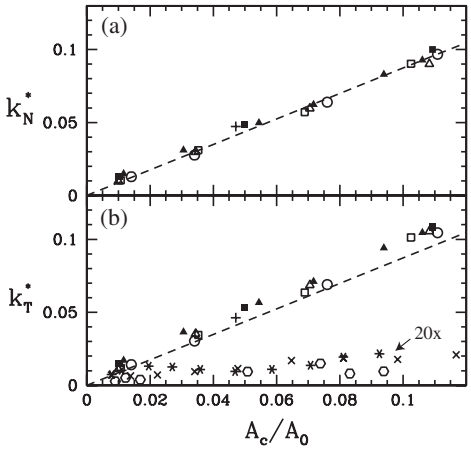

FIG. 3. The scaled (a) normal stiffness and (b) transverse stiffness as a function of A_c/A_0. Results for k^{Is} are shown for $H = 0.5$ (open symbols) and $H = 0.8$ (filled symbols) with $L = 189.2\sigma$ (circles), $L = 94.6\sigma$ (squares), or $L = 47.3\sigma$ (triangles). Pluses show GF results for $\nu = 0$. Total transverse stiffness k_T^{It}, multiplied by 20 to make visible, is shown for $L = 189.2\sigma$ and rigid surfaces with a square lattice, $d' = 0.37\sigma$, and $H = 0.5$ ($\times$) or $H = 0.8$ (hexagons), or a triangular lattice with $d' = 2^{1/6}\sigma$ and $H = 0.8$ ($*$). Dashed lines have slope 0.87.

This provides an estimate of the contribution that anharmonic effects may make to the stiffness of real materials at the rms slope used here.

The above results imply that the stiffness of elastic solids at fixed contact area is uniquely determined by the distribution of contacting points and not the surface roughness or load distribution. This conclusion may seem at odds with Eq. (2), since the contact area has no independent connection to load or surface roughness. The resolution is that variations in load and roughness cancel. If the response is linear, one can scale $h_{\rm rms}$ and F_N by the same factor and the contact area will be unchanged. Indeed one can combine Eqs. (1) and (2) to eliminate F_N:

$$k_N^* \equiv \frac{k_N^{Is}}{A_0 E'} \frac{h_{\rm rms}}{\sqrt{|\nabla h|^2}} = \frac{1}{\kappa\gamma} \frac{A_c}{A_0}. \tag{3}$$

For a self-affine surface, the ratio $h_{\rm rms}/\sqrt{|\nabla h|^2} \propto (l_{\rm max}/l_{\rm min})^H l_{\rm min}$ depends only on the small and large scale cutoffs in roughness, independent of the rms slope.

Figure 3(a) shows the scaled stiffness k_N^* vs area. The results were obtained by displacing atoms from their positions on the initial flat surface to eliminate anharmonic effects. Results for all systems collapse onto a common straight line, providing clear evidence for the direct connection between stiffness and contacting area. The slope is near unity as expected from the separate values of κ and γ.

All of our atomic simulations show $k_T^{Is}/k_N^{Is} \geq 1$. This is surprising given that Mindlin [19] and recent work [25] predict $k_T^I/k_N^I = 2(1-\nu)/(2-\nu) \leq 1$. However, this work assumed isotropic elasticity and the predicted ratio of unity is consistent with our GF results for an isotropic solid with $\nu = 0$. One measure of the anisotropy of the LJ crystal is that the ratio $c_{44}/E' \approx 0.57$, while it is $(1-\nu)/2 \leq 1/2$ for an isotropic solid. The higher shear modulus is consistent with a higher transverse stiffness than expected. In general, the total elastic energy stored in the interface is $\Sigma_q \vec{f}(-\vec{q})\vec{\vec{G}}(\vec{q})\vec{f}(\vec{q})/2$ where G is the Green's function matrix relating displacements to forces f [6]. The stiffness ratio can be obtained by averaging the diagonal components of $qG(\vec{q})$ corresponding to normal and transverse displacements over $\hat{q}$ and assuming the same power spectrum describes the respective forces. This ratio agrees with Mindlin's result for isotropic systems, and captures changes with crystal anisotropy.

As noted above, k_N^{Is} and k_T^{Is} reflect the stiffness associated with deformation inside the substrate at constant A_c, and there are additional interfacial stiffnesses k_N^{Ia} and k_T^{Ia} associated with the relative motion of atoms on opposing surfaces. The substrate and atomic compliances add in series, so the total interfacial stiffness $k_J^{It} = [1/k_J^{Is} + 1/k_J^{Ia}]^{-1}$ for $J = N$ or T. As in previous studies of single-asperity contacts [20,23,24], we find atomic-scale deformations have almost no effect on the total normal stiffness of multiasperity contacts, but qualitatively change the transverse stiffness.

The value of k_N^{Ia} is large because the repulsive forces on all contacting atoms add coherently to prevent interpenetration. One can estimate $k_N^{Ia} \sim A_c E'/\sigma$, assuming that the interfacial atoms act like a piece of the substrate with area A_c and height equal to the layer spacing $\sim\sigma$. This is larger than k_N^{Is} by a factor of order $h_{\rm rms}/\sigma\sqrt{|\nabla h|^2} \gg 1$, explaining why the total normal stiffness (Fig. 1) is consistent with the stiffness from compression of the elastic substrate alone (Fig. 2).

In contrast, the contributions to transverse stiffness from different atoms rarely add coherently. There is a direct

analogy to friction forces in single-asperity contacts [20,23,24], where the resistance to lateral sliding rises sublinearly with area unless the surfaces share a common periodicity. In Fig. 3(b) the total transverse interfacial stiffness is 2 orders of magnitude lower than k_T^{Is}. Results for different H are nearly the same, but the stiffness changes significantly with the lattice spacing d' and surface structure (square vs triangular). The transverse stiffness is also affected by $l_{\min}$, L and the interfacial potential.

Our k_T^{Ia} results for a wide range of parameters fall into two categories. The stiffness adds coherently in special cases, such as for commensurate surfaces with the same lattice structure. As for the normal stiffness, the contribution from k_T^{Ia} is then proportional to A_c and becomes irrelevant as system size L increases. For the more usual case where the different periodicity of the surfaces prevents coherent locking, k_T^{Ia} grows sublinearly with A_c and dominates the total stiffness at large L and A_c. Data for the cases in Fig. 3(b) satisfy $k_T^{Ia} = cA_c^{1/2}E'$, where E' is included to make c dimensionless and there are statistical fluctuations about the fit as new asperities contact. The value of c was independent of L and H, but larger for the square lattice than the triangular lattice. The substrate stiffness $k_T^{Is} \propto L^H A_c$ [Eq. (3)] grows more rapidly with L and A_c and thus becomes irrelevant in large systems.

Two aspects of the above results should be noted. The first is that the scaling $k_T^{Ia} \propto A_c^{1/2}$ is consistent with our observation that different connected patches contacted at random lateral registries because they could not displace laterally to optimize their position. Scaling theories predict that substrate stiffness prevents relative lateral displacements for L less than a correlation length that is estimated to be comparable to the size of macroscopic samples [26]. The second point is that the same arguments predict that the friction force scales as $A_c^{1/2}$ and this is not usually found in experiments. This suggests that another mechanism [24,27], such as debris or plasticity, may be important to both interfacial stiffness and friction in experimental samples. Further studies of interfacial stiffness may thus provide valuable information about friction mechanisms as well as explain the low ratio of transverse to normal stiffness frequently observed in experiment [10].

In conclusion, atomic-scale simulations were used to study contact between surfaces with roughness on a wide range of scales. The results for area and normal stiffness are consistent with Persson's continuum theory down to relatively small scales, even though the solid is not continuous or perfectly elastic. The area and internal stiffnesses of systems with a range of H, L, and ν show the linear scaling predicted in Eqs. (1)–(3) with nearly constant values of κ and γ. The internal stiffnesses were shown to depend only on the geometry of the contacting region. Atomic-scale displacements between contacting atoms have little effect on the normal stiffness, but can change the transverse stiffness by orders of magnitude. This sensitivity makes transverse stiffness a promising probe of the atomic-scale interactions that underlie friction.

Conversations with C. Campañá, M. H. Müser, and B. N. J. Persson are gratefully acknowledged. This material is based upon work supported by the Air Force Office of Scientific Research under Grant No. FA9550-0910232.

[1] F. P. Bowden and D. Tabor, *The Friction and Lubrication of Solids* (Clarendon Press, Oxford, 1986).
[2] J. A. Greenwood and J. B. P. Williamson, Proc. R. Soc. A **295**, 300 (1966).
[3] B. N. J. Persson, Phys. Rev. Lett. **87**, 116101 (2001).
[4] S. Hyun, L. Pei, J.-F. Molinari, and M. O. Robbins, Phys. Rev. E **70**, 026117 (2004).
[5] L. Pei, S. Hyun, J.-F. Molinari, and M. O. Robbins, J. Mech. Phys. Solids **53**, 2385 (2005).
[6] C. Campañá and M. H. Müser, Europhys. Lett. **77**, 38 005 (2007).
[7] D. G. Bellow and D. D. Nelson, Exp. Mech. **10**, 506 (1970).
[8] B. N. J. Persson, Phys. Rev. Lett. **99**, 125502 (2007).
[9] B. N. J. Persson, J. Phys. Condens. Matter **20**, 312 001 (2008).
[10] M. Gonzalez-Valadez, A. Baltazar, and R. S. Dwyer-Joyce, Wear **268**, 373 (2010).
[11] J. F. Archard, Proc. R. Soc. A **243**, 190 (1957).
[12] M. H. Müser, Phys. Rev. Lett. **100**, 055504 (2008).
[13] G. Carbone and F. Bottiglione, J. Mech. Phys. Solids **56**, 2555 (2008).
[14] S. Hyun and M. O. Robbins, Tribol. Int. **40**, 1413 (2007).
[15] C. Campañá, M. H. Müser, and M. O. Robbins, J. Phys. Condens. Matter **20**, 354 013 (2008).
[16] M. Benz, K. J. Rosenberg, E. J. Kramer, and J. N. Israelachvili, J. Phys. Chem. B **110**, 11 884 (2006).
[17] B. Lorenz and B. N. J. Persson, J. Phys. Condens. Matter **21**, 015003 (2009).
[18] C. Yang and B. N. J. Persson, Phys. Rev. Lett. **100**, 024303 (2008).
[19] R. D. Mindlin, J. Appl. Mech. **16**, 259 (1949).
[20] B. Luan and M. O. Robbins, Nature (London) **435**, 929 (2005).
[21] B. Luan and M. O. Robbins, Tribol. Lett. **36**, 1 (2009).
[22] S. J. Plimpton, J. Comput. Phys. **117**, 1 (1995); http://lammps.sandia.gov/.
[23] M. Hirano and K. Shinjo, Wear **168**, 121 (1993).
[24] M. H. Müser, L. Wenning, and M. O. Robbins, Phys. Rev. Lett. **86**, 1295 (2001).
[25] C. Campañá, B. N. J. Persson, and M. H. Müser, J. Phys. Condens. Matter **23**, 085001 (2011).
[26] B. N. J. Persson and E. Tosatti, Solid State Commun. **109**, 739 (1999).
[27] G. He, M. H. Müser, and M. O. Robbins, Science **284**, 1650 (1999).